



Designing and controlling the properties of transition metal oxide quantum materials

Charles Ahn¹, Andrea Cavalleri², Antoine Georges^{3,4}, Sohrab Ismail-Beigi¹✉, Andrew J. Millis^{4,5} and Jean-Marc Triscone⁶

This Perspective addresses the design, creation, characterization and control of synthetic quantum materials with strong electronic correlations. We show how emerging synergies between theoretical/computational approaches and materials design/experimental probes are driving recent advances in the discovery, understanding and control of new electronic behaviour in materials systems with interesting and potentially technologically important properties. The focus here is on transition metal oxides, where electronic correlations lead to a myriad of functional properties including superconductivity, magnetism, Mott transitions, multiferroicity and emergent behaviour at picoscale-designed interfaces. Current opportunities and challenges are also addressed, including possible new discoveries of non-equilibrium phenomena and optical control of correlated quantum phases of transition metal oxides.

Quantum materials such as complex oxides display cooperative effects involving the interplay of multiple degrees of freedom (charge, spin, orbital, lattice) that lead to a wide variety of electronic phases and properties. These effects raise fundamental scientific questions and provide potentially useful functionalities. The tight interplay between different electronic phases is both an opportunity and a challenge for materials design and property control. Notable progress has recently been achieved in two experimental directions: synthesis and growth of transition metal oxide quantum materials, and advanced characterization and spectroscopy of the resulting electronic properties. At the same time, theory is reaching the stage where some properties can be predicted quantitatively, and some materials can be designed de novo.

Continued development of materials synthesis techniques, in particular thin-film deposition¹ and molecular-beam epitaxy methods², has allowed for the construction of artificially layered materials with both atomic specificity and picometre precision and led to fine control of electronic properties. The ability to fabricate materials a single atomic layer at a time permits the control of fundamental parameters (for example, electronic bandwidth, splitting between energy levels of different orbitals, screening) to achieve specific electronic properties. However, there are still appreciable challenges to overcome, including refined control of oxygen stoichiometry, minimization of point and antisite defects, low-temperature growth, and control over heterostructuring of nominally incompatible constituent materials.

The ability to fabricate materials with such precision has spurred the development of instrumentation and measurement techniques. Advances in scanning transmission electron microscopy (STEM)³ and synchrotron crystal truncation rod diffraction analysis⁴ have enabled the determination of materials structure down to the picometre level, even for the small sample volumes of ultrathin films and heterostructures. Developments in photon-based spectroscopies, such as resonant inelastic X-ray scattering⁵ and X-ray photon correlation spectroscopy⁶, have added to the battery of high-resolution spectroscopies, such as angle-resolved photoelectron

spectroscopy (ARPES)⁷ and scanning tunnelling microscopy⁸. New avenues have also been opened towards the exploration and control of quantum materials in out-of-equilibrium conditions, for example using intense ultrashort light pulses and time-resolved structural determination via free-electron lasers⁹.

In this context, theoretical guidance on the materials that should be synthesized and the measurements that should be made is critical. Conversely, careful comparison with high-resolution experiments can validate the assumptions and approximations underpinning theories of complex quantum materials. Figure 1 shows the synergistic interplay between theory and experiment that drives progress in the field.

Theoretically, describing strongly interacting quantum many-particle systems is challenging. The exponentially large Hilbert space and the quantum entanglement of many degrees of freedom make an exact theoretical treatment impossible. For materials in which electronic correlations are relatively weak, computational methods based on the single-particle framework of density functional theory (DFT) have proven remarkably successful both in understanding properties and in providing guidance towards materials design and engineering¹⁰.

However, in materials with strong electronic correlations, such as transition metal oxides with partially filled *d* shells, the electronic excitation spectra cannot be described reliably within the band-theory paradigm and require the development of theoretical approaches that directly address correlations. Dynamical mean-field theory (DMFT)^{11,12} has emerged as a widely used method going beyond the limitations of DFT, allowing for quantitative calculations of many properties of materials with strong correlations, thanks to continued developments in computational methodologies.

This Perspective presents an overview of theoretical progress, in relation to ongoing efforts in materials design and novel spectroscopies. We highlight a few materials families where the interplay of theory and experiment has been successful. We then discuss ongoing challenges on the theoretical as well as the experimental side. Connections are drawn to the areas of quantum chemistry, ultrafast

¹Yale University, New Haven, CT, USA. ²Max Planck Institute for the Structure and Dynamics of Matter, Hamburg, Germany. ³Collège de France, Paris, France. ⁴CCQ-Flatiron Institute, New York, NY, USA. ⁵Columbia University, New York, NY, USA. ⁶University of Geneva, Geneva, Switzerland.

✉e-mail: sohrab.ismail-beigi@yale.edu

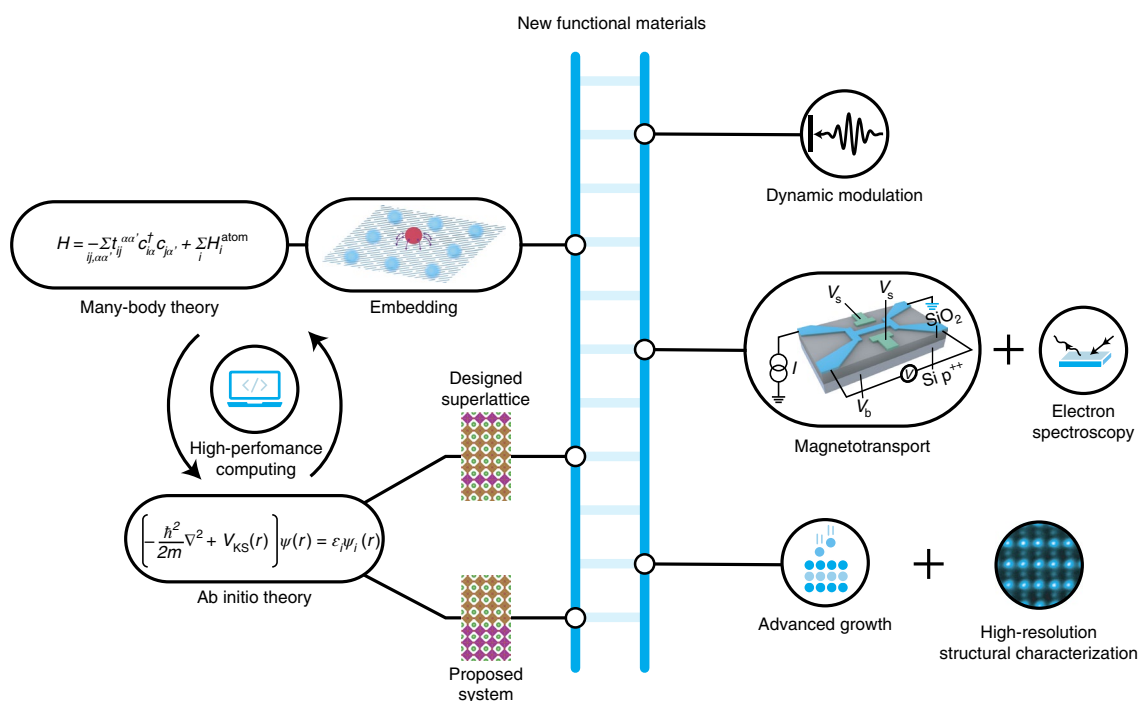


Fig. 1 | Interplay of theory and experiment. Schematic showing the interplay between theory and experiment when proposing, measuring, understanding and designing electronic properties of quantum materials. Each rung of the ladder represents a certain class of methods, and knowledge and materials complexity are enhanced as the ladder is ascended. On the left-hand side of the ladder, key theoretical tools are highlighted, including DFT-based electronic structure theory (exemplified in the ‘Ab initio theory’ box by the single-particle Kohn–Sham (KS) eigenvalue equations, involving the self-consistently determined Kohn–Sham potential V_{KS} , that provide, upon solving the equations, the energy ϵ_i and wave function $\psi_i(r)$ of each electron separately), as well as the inclusion of electronic correlations through many-body embedding methods such as DMFT (represented by the Hubbard model Hamiltonian in the ‘Many-body theory’ box describing electron tunnelling processes with strength $-t_{ij}^{aa'}$ between orbital a on atom i and orbital a' on atom j together with localized electron–electron interactions H_i^{atom} on each atom i). The two levels of methods are self-consistently coupled (arrows). Implementing this theoretical framework requires the development of advanced algorithms and software and the use of high-performance computing. On the right, critical experimental approaches are indicated: layer-by-layer synthesis using molecular-beam epitaxy, synchrotron X-ray characterization of atomic-scale structure, magnetotransport measurements and several spectroscopies, as well as pump–probe dynamic control. On the first rung, theorists identify and model an interfacial system using first-principles DFT calculations. Next, experimental structural characterization describes the actual interfacial structural motifs. This leads theorists to use DFT to design a new superlattice heterostructure incorporating the key observed structural motifs that should lead to new electronic states. Experiments on this superlattice reveal unexpected magnetotransport or spectroscopic results that are not comprehensible with independent-electron band structures, calling for the use of many-body electronic structure methods to account for electronic correlations and to describe emergent collective phases. Pump–probe experiments offer a pathway for the dynamic control of these emergent electronic properties.

dynamics and strong light–matter interactions, as well as to materials beyond the Mott-correlated-electron paradigm.

Theoretical background: from weak to strong correlations

In the absence of interactions between electrons, the quantum state of a multielectron system is constructed by finding individual states for a single electron and populating these states according to Fermi statistics. In a periodic solid, these single-electron states are Bloch waves, organized into energy bands — hence the term band theory.

Once interactions are introduced, the motions of different electrons become correlated and their states become entangled. In practice, if the correlations are weak the band-theory picture is still a good approximation, provided that, when solving for each single-electron state, we include the averaged effect of the other electrons via some mean-field approximation. This approach is best exemplified by DFT, which in principle provides the exact ground-state energy and electron density. Examples of successes for DFT-based methods include the study and/or design of ferroelectric¹³ and multiferroic¹⁴ materials and predictions of hydrogen-based superconductors under high pressure¹⁵. Despite DFT successes, there are problems

even for weak correlations. The exact DFT energy functional is not known and there is an ongoing effort to improve the approximate functionals now in use. More fundamentally, DFT provides only a single-electron mean-field approximation of excited states, often in disagreement with experimental spectroscopic measurements. Perturbative treatments of electron–electron interactions, as implemented for example in the GW approximation¹⁶, can produce quantitatively accurate excitation spectra for weakly correlated materials. However, for wide classes of materials, non-perturbative methods are needed to obtain both the correct ground state and the observed excitation spectrum. These materials are referred to as strongly correlated.

It should be emphasized that strong correlation is not identical to strong interaction. For example, when electron–electron repulsions become very strong, the physics is often simply that of localized electrons avoiding each other in real space and the wave function may sometimes be approximated as a simple product form — see, for example, ref. 17. The strong-correlation problem can emerge in two cases. In the highly localized regime, strong quantum fluctuations associated, for example, with spin- $\frac{1}{2}$ degrees of freedom and geometrical frustration can give rise to ‘spin-liquid’ behaviour not

understandable in terms of simple product wave functions. Moving beyond strong localization, the intermediate regime where electrons ‘hesitate’ between delocalized behaviour (electrons behaving as waves) and localized behaviour (electron behaving as particles) is especially challenging. This is the case in materials such as transition metal oxides close to a Mott metal–insulator transition¹⁸ or rare-earth and actinide compounds¹⁹. Such quantum materials are difficult to describe using a one-electron picture.

Electronic structure calculations with DMFT have proven successful in this intermediate regime. The DMFT approach starts with a description of the many-body electronic state of the individual atoms. Subject to interactions such as Coulomb repulsions and the intra-atomic exchange (Hund’s coupling), the electrons of an incomplete *d* or *f* shell organize into many-body eigenstates known as ‘atomic multiplets’. When atoms are brought together to form an extended solid, electron hopping events lead to local changes in the multiplet configuration that each atom adopts in time and space. DMFT describes the history of quantum fluctuations between these multiplet configurations. At high energies, only a few configurations are relevant, and the excitations of the system are well described in terms of real-space transitions between atomic multiplets — such as ‘Hubbard bands’, which are valence transitions corresponding to the addition or removal of one electron in the atomic shell. At low energies, wave-like quasiparticle excitations best described in momentum space emerge as a result of the superposition of a large number of local configurations. The theory has been successfully combined with state-of-the-art electronic structure methods such as DFT or GW (refs. ^{18,20,21}), allowing for a realistic description of the electronic structure of quantum materials with strong electronic correlations. This ability to describe both atomic-like excitations and low-energy quasiparticles in a chemically realistic context and hence to solve the localized/delocalized, particle-like/wave-like conundrum is the main success of DMFT.

While the concept underlying the DMFT approximation is general, existing implementations involve strong locality assumptions. Typically, dynamical interactions and correlations are treated only one site at a time. Extensions and generalizations of the quantum embedding concept that relax this restriction are under development^{22–26}. Promising theoretical approaches not based on embedding are currently subjects of active research, including diffusion and auxiliary field quantum Monte Carlo methods²⁷ and density-matrix renormalization-group/tensor network methods²⁸, with recent applications to molecular systems and quantum-chemistry-based methods^{29,30}. Given space constraints and because these methods have not yet been applied to a wide range of materials, we will not discuss them further here.

Nickelates and the electron–lattice interplay

The rare-earth nickelates, with formula $RNiO_3$, are a prominent example of a family of compounds displaying (with the notable exception of $LaNiO_3$) a metal–insulator transition as temperature is reduced³¹. Concomitant with the entry into the insulating phase is a symmetry-lowering structural transition to a two-sublattice bond disproportionated structure with alternately expanded and contracted NiO_6 octahedra.

This electronic transition can be visualized in real space using for instance scanning near-field optical microscopy³² and photo-emission electron microscopy (PEEM)³³. Figure 2 shows PEEM maps revealing the temperature evolution of metallic and insulating domains across the metal–insulator transition and resistivity versus temperature for a representative $NdNiO_3$ film.

The $RNiO_3$ materials crystallize in the perovskite structure, a network of corner-sharing NiO_6 octahedra with the rare-earth atoms occupying the spaces in between. As the rare-earth size is increased the Ni–O–Ni bond angle is straightened and the orbital overlap is enhanced between the Ni *d* states and the O *p* states. This

increases the bandwidth and, in turn, decreases the metal–insulator transition temperature (T_{MI}).

Usual valence counting for an ABO_3 perovskite with a trivalent A^{3+} cation assigns an O^{2-} state to oxygen, implying that Ni is in the $3+$ (d^7) state. This valence assignment is problematic for two reasons: Ni d^7 involves one electron in the twofold-degenerate e_g -symmetry orbital manifold, so this configuration should be highly susceptible to Jahn–Teller distortions, which are not observed. In addition, the d^7 configuration is not susceptible to the observed bond disproportionation because this would imply an electronic disproportionation from d^7-d^7 to d^8-d^6 , which is disfavoured by the Hubbard U . As recognized early on³⁴, Ni is nearly as electronegative as oxygen in these compounds, implying that the Ni valence is closer to $2+$ and the dominant configuration in the wave function is d^8L , with L denoting an oxygen ligand hole. In this configuration, Hund’s first rule strongly favours a high-spin, approximately charge-symmetric configuration for the Ni, explaining the lack of Jahn–Teller distortions and instead a bond and charge disproportionation (two parallel spins every other site).

In the insulating phase, the electronic disproportionation can be viewed schematically as $d^8L + d^8L \rightarrow d^8 + d^8L^2$, in which the d^8 octahedra carry a magnetic moment close to spin $S=1$ while the d^8L^2 octahedra have a vanishing moment³⁵. This interplay of correlation and bonding effects is naturally captured by DMFT calculations³⁶, which have confirmed the picture and provided an understanding of the metal–insulator transition as a ‘site-selective Mott transition’, in which the Mott phenomenon takes place on the d^8 sites, while the d^8L^2 sites undergo a Kondo-like screening.

Despite the more realistic nature of the ligand-hole picture, the essential physics of the $RNiO_3$ metal–insulator transition is well captured by a low-energy description of the electronic structure that retains only the strongly hybridized Ni $3d/O$ $2p$ Wannier states forming the frontier e_g bands near the Fermi level³⁷. This low-energy effective model must involve strongly screened interactions.

The nickelates, like many other correlated materials, exhibit a close interplay between electronic instabilities and lattice distortions. Recently, theoretical studies in the context of nickelates have revealed the key parameters controlling this interplay³⁸. These distortions modify the electronic structure (for example, bandwidth, susceptibility to electronic disproportionation) via tuning of the Ni–O–Ni bond angle, which can be modified in epitaxial heterostructures by strain, substrate orientation and ultrafast light pulses, achieving control of the metal–insulator transition in nickelates³⁹.

The active and ongoing feedback between theory, measurement, materials synthesis and characterization has pushed the frontier of state-of-the-art science on all sides. This has enabled a much deeper understanding of many-body electronic structure, metal–insulator transitions and approaches to engineering functional properties.

Ruthenates: Hund’s metals and non-equilibrium steady states

The different members of the Ru oxide based Ruddlesden–Popper perovskite series $X_{n+1}Ru_nO_{3n+1}$ (with $X = Sr, Ca, Ba$) display a wide diversity of unusual behaviours depending both on X and on n . The three-dimensional ($n = \infty$) compound $SrRuO_3$ is a ferromagnetic metal with possible applications to spintronics whereas $CaRuO_3$ remains a paramagnetic metal down to the lowest temperatures. The single-layer ($n = 1$) compound Sr_2RuO_4 is a remarkable superconductor⁴⁰ while Ca_2RuO_4 exhibits a correlation-driven metal–insulator transition involving a rich interplay between orbital, charge and lattice degrees of freedom⁴¹. Bilayer ($n = 2$) $Sr_3Ru_2O_7$ displays a quantum critical endpoint with associated formation of an electronic nematic phase under an applied magnetic field⁴² while bilayer $Ca_3Ru_2O_7$ is a ‘ferroelectric-like metal’ (that is, one with broken inversion symmetry) with interesting magnetic phases and an incipient Mott transition revealed by modest Ti substitution on the

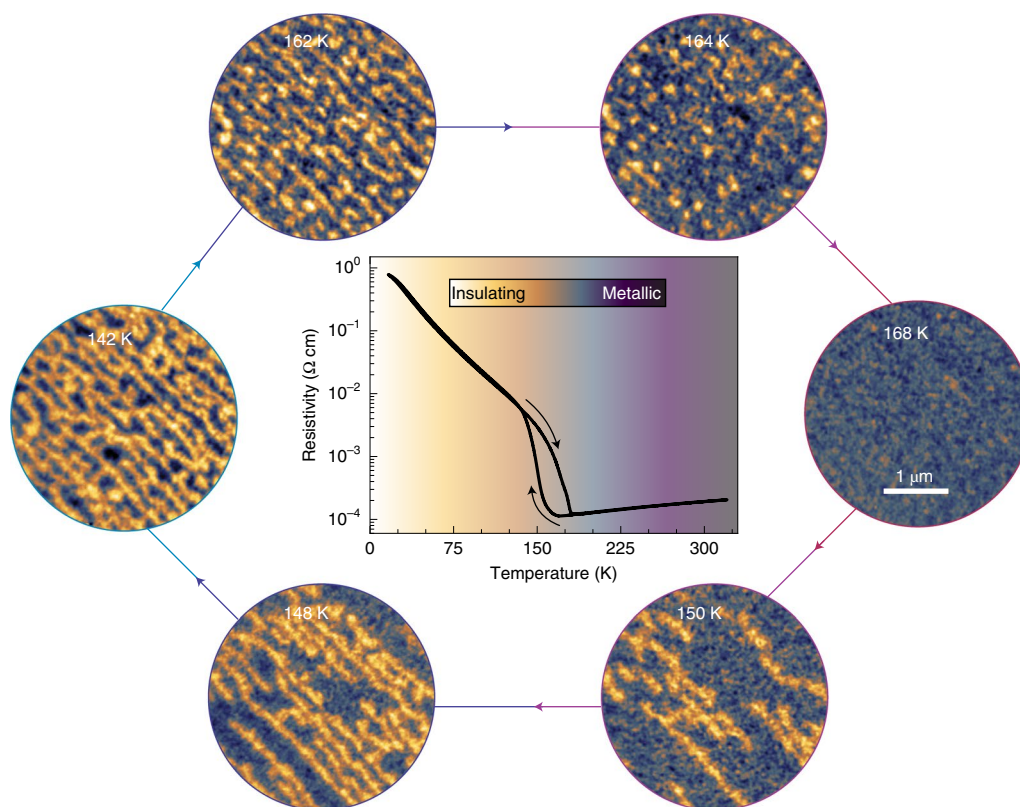


Fig. 2 | Metal-insulator transition in nickelates. Temperature evolution of metallic and insulating domains across the metal-insulator transition and resistivity versus temperature for a 30-unit-cell-thick (001) NdNiO₃ film grown on NdGaO₃. Around the inset: PEEM maps of the insulating and metallic regions (dark blue is metallic, yellow insulating) obtained from differences in the metallic and insulating state local X-ray absorption spectra obtained at each location of the map. During each thermal cycle the insulating domains nucleate and grow on cooling, while they gradually disappear on warming. Inset: resistivity versus temperature, revealing, as seen in the PEEM maps, hysteresis, signature of a first-order phase transition. Credit: figure adapted with permission from ref. ³³, Springer Nature Ltd.

Ru site⁴³. Both the $n=1$ and $n=2$ Ca compounds reveal remarkable current-driven insulator-metal transitions⁴⁴. The challenge of unravelling the dependence of physical properties on X , n , strain and current has stimulated the development of both experimental and theoretical techniques. For example, the variation of magnetic properties across the series going from CaRuO₃ to SrRuO₃ and then to BaRuO₃ has provided both a confirmation of the DMFT approach and insights into the physics of ferromagnetism^{45,46}.

Sr₂RuO₄ is of particular interest because large single crystals with outstanding purity can be synthesized, allowing for essentially all of the experimental probes in the community's toolbox to be successfully used and enabling precise comparisons of quantum many-body calculations with experiments⁴⁷. At very high temperatures, the material is a 'bad metal', with resistivity exceeding the Mott-Ioffe-Regel limit⁴⁸. An intermediate-temperature 'strange-metal' regime characterized by quasilinear resistivity, an enhanced Seebeck coefficient and a temperature-dependent Hall coefficient separates the bad-metal regime from a low- T (<25 K) Fermi liquid with enhanced quasiparticle effective masses⁴⁹. A theoretical understanding of the main features of these normal-state properties has been achieved. Of particular note are ultrahigh-resolution laser ARPES experiments that have provided a direct determination of the electronic self-energy⁴⁷, enabling an unambiguous test of the locality ansatz assumed in the DMFT approach.

These studies have revealed that the key driver of the physics of the ruthenates is the on-site Hund's coupling⁵⁰, marking the ruthenates as members of the broad class of 'Hund's metals', which also includes the iron-based superconductors. Studies^{51,52} have revealed

that a hallmark of these materials is a subtle interplay between local spin and orbital fluctuations, associated with distinct temperature scales.

Ca₂RuO₄ is a bad metal at high temperatures, but below $T \sim 350$ K it undergoes a transition into a non-magnetic insulating state, followed by antiferromagnetic ordering at $T_N \approx 140$ K. The crystal symmetry does not change across the transition, but an orbital disproportionation appears in which the Ru d_{xy} orbital becomes fully occupied and the d_{xz}/d_{yz} orbitals correspondingly become half filled and prone to Mott insulating behaviour, while the RuO₆ octahedra undergo a compression along the c axis. The transition is found to be remarkably sensitive to epitaxial constraints⁵³, with thin films of Ca₂RuO₄ grown epitaxially on NdGaO₃ (+0.3% strain) and LaSrAlO₄ (-0.48% strain) remaining insulating up to 550 K while films grown on NdAlO₃ (-3.0% strain) remain metallic down to the lowest temperature. Only films grown on LaAlO₃ (-1.6% strain) exhibit a transition to a weakly insulating phase at $T \approx 20$ K. All of these features of Ca₂RuO₄ have been understood in the context of the DFT + DMFT approach⁵⁴⁻⁵⁶.

Superconductivity in non-cuprate oxides: search and discovery

The 1986 discovery of superconductivity in derivatives of La_{2-x}Ba_xCuO₄ opened an entirely new field of research and launched a search for other superconducting oxides. One early success was the 1994 discovery of superconductivity in Sr₂RuO₄, a structural analogue of La₂CuO₄ with, however, strikingly different local physics driven by multiorbital Hund's, rather than single-orbital Mott,

correlations. The search for superconductivity in single-orbital Mott systems initially focused on Ni-based materials⁵⁷. It was proposed⁵⁸ that metallic LaNiO₃ could be made superconducting by using quantum confinement and strain to lift the degeneracy of the two quarter-filled degenerate e_g bands, thereby producing one half-filled $d_{x^2-y^2}$ e_g band with two-dimensional character in direct analogy with the cuprates. This prediction sparked the improvement of sophisticated orbital-sensitive probes for ultrathin films⁵⁹, spurred the development of DFT + DMFT and led to experiments on LaNiO₃-based heterostructures^{60,61}. However, in nickelate Ni³⁺ superlattices, the d^8 nature of the Ni³⁺ ground state strongly limits the degree of orbital differentiation⁶². Theoretically designed superlattices featuring substantial electron transfer to the Ni possess large orbital splittings: strong local fields elongate apical Ni–O bonds and create robust e_g orbital differentiation on Ni²⁺ (d^8) with a record orbital polarization of 50% (ref. 63). However, direct analogy with cuprates requires further orbital polarization and electron doping towards Ni⁺. The quest for nickelate superconductivity was rewarded with the breakthrough discovery⁶⁴ that Nd_{0.8}Sr_{0.2}NiO₂ superconducts with a critical temperature of up to 15 K with an unusual Ni⁺ (d^9) state. This new family of nickelate superconductors is currently under intensive experimental and theoretical study, with a key question being whether they are governed by single-orbital Mott or multiorbital Hund's physics.

Ultrafast control and new spectroscopies

Non-equilibrium phenomena have also been increasingly explored in correlated oxides, with notable advances both in experiment and in theory. Especially fruitful have been those experimental studies in which terahertz-frequency radiation was used to selectively drive collective modes nonlinearly. These optical control methods have opened up an entirely new toolset to control functionality at high speeds, and contrast with more traditional linear optical spectroscopies that expose collective equilibrium behaviour without perturbing the state of the material. Nonlinear excitation makes it now possible to control as opposed to simply observe the materials state.

Coherent control of lattice dynamics^{65,66} has been especially fruitful, in its applications to steer electronic⁶⁷, magnetic⁶⁸ and ferroelectric orders⁶⁹, where selective distortions of certain bond angles have been shown to change the delicate balance between different interactions and the macroscopic functional properties. Advances in these areas have also been aided by new probing methods, including ultrafast x-ray free-electron lasers, which make it possible to quantify these dynamics at femtosecond time resolution. Extensive theoretical work has followed, with many proposals for achieving nonlinear phonon control in materials^{70,71}.

Arguably the most surprising results have emerged in driven unconventional superconductors, in which signatures of induced, non-equilibrium superconductivity were reported for temperatures far in excess of the thermodynamic critical temperature T_c (ref. 72). These experiments have initially focused on the targeted suppression of those competing orders that inhibit superconductivity at equilibrium, or more generally on transient lattice deformations and their coupling to the electronic structure⁷³ (Fig. 3). Further work has broadened the scope of this class of phenomena, with reported non-equilibrium superconductivity in organic compounds such as K₃C₆₀ (ref. 74) and ET₂Cu[N(CN)₂]Br (ref. 75), indicating that the underlying mechanisms must be more general than originally envisaged.

Theoretical work has then increasingly explored genuinely dynamical phenomena in which the drive creates time-dependent Hamiltonian parameters, rather than switching into quasiequilibrium states. For example, the role of effective attractive electronic interactions (negative U) have been brought to the fore in vibrational excited states for molecular solids⁷⁶, as well as the role of parametric interactions in driven oxides, which predict cooling

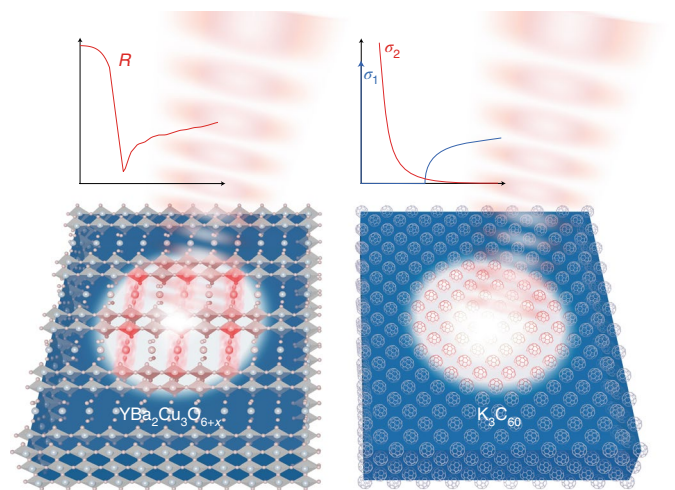


Fig. 3 | Non-equilibrium superconductivity in YBa₂Cu₃O_{6+x} and in K₃C₆₀. Optically enhanced non-equilibrium superconductivity in YBa₂Cu₃O_{6+x} and in K₃C₆₀. The material is irradiated by a train of terahertz pulses (light red), which are tuned to the frequency of lattice vibrations in the cuprates or of a local vibrational mode of the C₆₀ molecule. The irradiated area acquires the low-frequency optical properties of the equilibrium low-temperature superconducting state at temperatures much higher than T_c . These properties are evidenced by the transient appearance of a plasma edge in the c -axis reflectivity of YBa₂Cu₃O_{6+x} ($R(\omega)$ — red curve — left-hand graph). For K₃C₆₀, transient superconductivity is evidenced by a gapping in the real part of the optical conductivity ($\sigma_1(\omega)$ — blue curve — right-hand graph) and a divergent imaginary part of the same complex function ($\sigma_2(\omega)$ — red curve — right-hand graph).

of thermal fluctuations⁷⁷ or synchronization of phase-incoherent superconductors⁷⁸. These and other similar studies may not have yet provided a comprehensive understanding of the microscopic physics of optically stimulated order in quantum materials, but they are prompting new thinking on strong correlations in driven settings, providing a language to describe a new generation of phenomena and possibly high-speed device applications for quantum materials.

Outlook

As the examples given in this article show, the past few years have seen notable progress in our ability to synthesize, measure, calculate and control the properties of materials with strong electronic correlations in bulk, heterostructure and ultrathin-film forms. Key emergent themes include the non-trivial interplay between electronic and lattice properties, the tension between Mott and Hund's correlations, and the importance of non-equilibrium drive as both a novel spectroscopy and a new form of control of materials properties. These successes raise important challenges for the future. Extending the understanding achieved in the nickelates and ruthenates to other oxides and further to other classes of materials including (possibly twisted) transition metal dichalcogenides, and also addressing topological and collective mode behaviour, are important scientific opportunities. The novel non-equilibrium states created by new generations of dynamical experiments call out for understanding.

On the theoretical side, the primary workhorse enabling the new class of systematic experiment–theory comparisons has been the density functional plus dynamical mean-field methodology. While there is now substantial a posteriori justification in terms of theory–experiment agreement, especially for multiorbital transition metal oxides, further development of the theoretical framework is required to bring this methodology to the same level of flexibility and usefulness that the density functional plus GW formalism has

achieved for weakly correlated materials. Among the challenging areas under active theoretical development are the following: development of more efficient methods for calculating the two-particle correlators needed for transport, susceptibility and other response functions; describing the very low energy scales typically needed for studies of superconductivity, including electron–phonon interactions; extending the capabilities further within the regime of dynamics; and making the methods more usable and user friendly, so that they can for example guide materials design and synthesis efforts⁷⁹.

Strong locality assumptions are fundamental to the DMFT methodologies currently in active use. Successful experiment–theory comparisons such as those reported above have provided a posteriori justification in some cases. Among the key theoretical challenges for the future are going beyond the locality assumptions to permit the inclusion of longer-range interactions and fluctuations beyond the local approximation within the DMFT/embedding scheme, and developing other methods that can treat strong correlations to permit the same level of theory–experiment comparison.

Received: 8 July 2020; Accepted: 17 March 2021;

Published online: 3 May 2021

References

- Choi, W. S. et al. Atomic layer engineering of perovskite oxides for chemically sharp heterointerfaces. *Adv. Mater.* **24**, 6423–6428 (2012).
- Lei, Q. et al. Constructing oxide interfaces and heterostructures by atomic layer-by-layer laser molecular beam epitaxy. *npj Quantum Mater.* **2**, 10 (2017).
- Muller, D. A. Structure and bonding at the atomic scale by scanning transmission electron microscopy. *Nat. Mater.* **8**, 263–270 (2009).
- Disa, A. S., Frederick, J. W. & Charles, H. A. High-resolution crystal truncation rod scattering: application to ultrathin layers and buried interfaces. *Adv. Mater. Interfaces* **7**, 1901772 (2020).
- Ament, L. J. P., van Veenendaal, M., Devereaux, T. P., Hill, J. P. & van den Brink, J. Resonant inelastic x-ray scattering studies of elementary excitations. *Rev. Mod. Phys.* **83**, 705 (2011).
- Kukreja, R. et al. Orbital domain dynamics in magnetite below the Verwey transition. *Phys. Rev. Lett.* **121**, 177601 (2018).
- Damascelli, A., Hussain, Z. & Shen, Z.-X. Angle-resolved photoemission studies of the cuprate superconductors. *Rev. Mod. Phys.* **75**, 473–541 (2003).
- Huang, B.-C. et al. Mapping band alignment across complex oxide heterointerfaces. *Phys. Rev. Lett.* **109**, 246807 (2012).
- Dean, M. P. M. et al. Ultrafast energy- and momentum-resolved dynamics of magnetic correlations in the photo-doped Mott insulator Sr_2IrO_4 . *Nat. Mater.* **15**, 601–605 (2016).
- Zhong, W., Vanderbilt, D. & Rabe, K. M. First-principles theory of ferroelectric phase transitions for perovskites: the case of BaTiO_3 . *Phys. Rev. B* **52**, 6301–6312 (1995).
- Georges, A., Kotliar, G., Krauth, W. & Rozenberg, M. J. Dynamical mean-field theory of strongly correlated fermion systems and the limit of infinite dimensions. *Rev. Mod. Phys.* **68**, 13–125 (1996).
- Kotliar, G. et al. Electronic structure calculations with dynamical mean-field theory. *Rev. Mod. Phys.* **78**, 865–951 (2006).
- Neaton, J. B. & Rabe, K. M. Theory of polarization enhancement in epitaxial $\text{BaTiO}_3/\text{SrTiO}_3$ superlattices. *Appl. Phys. Lett.* **82**, 1586–1588 (2003).
- Lee, J. H. et al. A strong ferroelectric ferromagnet created by means of spin–lattice coupling. *Nature* **466**, 954–958 (2010).
- Drozdov, A. P., Erements, M. I., Troyan, I. A., Ksenofontov, V. & Shylin, S. I. Conventional superconductivity at 203 kelvin at high pressures in the sulfur hydride system. *Nature* **525**, 73–76 (2015).
- Onida, G., Reining, L. & Rubio, A. Electronic excitations: density-functional versus many-body Green's-function approaches. *Rev. Mod. Phys.* **74**, 601–659 (2002).
- Varignon, J., Bibes, M. & Zunger, A. Origin of band gaps in 3d perovskite oxides. *Nat. Commun.* **10**, 1658 (2019).
- Imada, M., Fujimori, A. & Tokura, Y. Metal–insulator transitions. *Rev. Mod. Phys.* **70**, 1039–1263 (1998).
- Stewart, G. R. Heavy-fermion systems. *Rev. Mod. Phys.* **56**, 755–787 (1984).
- Biermann, S., Aryasetiawan, F. & Georges, A. First-principles approach to the electronic structure of strongly correlated systems: combining the GW approximation and dynamical mean-field theory. *Phys. Rev. Lett.* **90**, 086402 (2003).
- Sun, P. & Kotliar, G. Extended dynamical mean-field theory and GW method. *Phys. Rev. B* **66**, 085120 (2002).
- Rusakov, A. A., Iskakov, S., Tran, L. N. & Zgid, D. Self-energy embedding theory (SEET) for periodic systems. *J. Chem. Theory Comput.* **15**, 229–240 (2018).
- Knizia, G. & Chan, G. K.-L. Density matrix embedding: a simple alternative to dynamical mean-field theory. *Phys. Rev. Lett.* **109**, 186404 (2012).
- Zhu, T., Cui, Z.-H. & Chan, G. K.-L. Efficient formulation of ab initio quantum embedding in periodic systems: dynamical mean-field theory. *J. Chem. Theory Comput.* **16**, 141–153 (2019).
- Nilsson, F., Boehnke, Werner, L. P. & Aryasetiawan, F. Multitier self-consistent GW + EDMFT. *Phys. Rev. Mater.* **1**, 043803 (2017).
- Choi, S., Semon, P., Kang, B., Kutepov, A. & Kotliar, G. ComDMFT: a massively parallel computer package for the electronic structure of correlated-electron systems. *Comput. Phys. Commun.* **244**, 277–294 (2019).
- Foulkes, W. M. C., Mitas, L., Needs, R. J. & Rajagopal, G. Quantum Monte Carlo simulations of solids. *Rev. Mod. Phys.* **73**, 33–83 (2001).
- Schollwöck, U. The density-matrix renormalization group. *Rev. Mod. Phys.* **77**, 259–315 (2005).
- McClain, J., Sun, Q., Chan, G. K.-L. & Berkelbach, T. C. Gaussian-based coupled-cluster theory for the ground-state and band structure of solids. *J. Chem. Theory Comput.* **13**, 1209–1218 (2017).
- Booth, G. H., Thom, A. J. W. & Alavi, A. Fermion Monte Carlo without fixed nodes: a game of life, death, and annihilation in Slater determinant space. *J. Chem. Phys.* **131**, 054106 (2009).
- Medarde, M. L. Structural, magnetic and electronic properties of RNiO_3 perovskites (R = rare earth). *J. Phys. Condens. Matter* **9**, 1679–1707 (1997).
- Post, K. W. et al. Coexisting first- and second-order electronic phase transitions in a correlated oxide. *Nat. Phys.* **14**, 1056–1061 (2018).
- Mattoni, G. et al. Striped nanoscale phase separation at the metal–insulator transition of heteroepitaxial nickelates. *Nat. Commun.* **7**, 13141 (2016).
- Mizokawa, T., Khomskii, D. I. & Sawatzky, G. A. Spin and charge ordering in self-doped Mott insulators. *Phys. Rev. B* **61**, 11263–11266 (2000).
- Mazin, I. I. et al. Charge ordering as alternative to Jahn–Teller distortion. *Phys. Rev. Lett.* **98**, 176406 (2007).
- Park, H., Millis, A. J. & Marianetti, C. A. Site-selective Mott transition in rare-earth-element nickelates. *Phys. Rev. Lett.* **109**, 156402 (2012).
- Seth, P. et al. Renormalization of effective interactions in a negative charge transfer insulator. *Phys. Rev. B* **96**, 205139 (2017).
- Peil, O. E., Hampel, A., Ederer, C. & Georges, A. Mechanism and control parameters of the coupled structural and metal–insulator transition in nickelates. *Phys. Rev. B* **99**, 245127 (2019).
- Middey, S. et al. Physics of ultrathin films and heterostructures of rare-earth nickelates. *Annu. Rev. Mater. Res.* **46**, 305–334 (2016).
- Mackenzie, A. P., Scaffidi, T., Hicks, C. W. & Maeno, Y. Even odder after twenty-three years: the superconducting order parameter puzzle of Sr_2RuO_4 . *npj Quantum Mater.* **2**, 40 (2017).
- Nakatsuji, S. et al. Heavy-mass Fermi liquid near a ferromagnetic instability in layered rhenates. *Phys. Rev. Lett.* **90**, 137202 (2003).
- Fradkin, E., Kivelson, S. A., Lawler, M. J., Eisenstein, J. P. & Mackenzie, A. P. Nematic Fermi fluids in condensed matter physics. *Annu. Rev. Condens. Matter Phys.* **1**, 153–178 (2010).
- Lei, S. et al. Observation of quasi-two-dimensional polar domains and ferroelastic switching in a metal, $\text{Ca}_3\text{Ru}_2\text{O}_7$. *Nano Lett.* **18**, 3088–3095 (2018).
- Nakamura, F. et al. Electric-field-induced metal maintained by current of the Mott insulator Ca_2RuO_4 . *Sci. Rep.* **3**, 2536 (2013).
- Dang, H. T., Mravlje, J., Georges, A. & Millis, A. J. Electronic correlations, magnetism, and Hund's rule coupling in the ruthenium perovskites SrRuO_3 and CaRuO_3 . *Phys. Rev. B* **91**, 195149 (2015).
- Han, Q., Dang, H. T. & Millis, A. J. Ferromagnetism and correlation strength in cubic barium ruthenate in comparison to strontium and calcium ruthenate: a dynamical mean-field study. *Phys. Rev. B* **93**, 155103 (2016).
- Tamai, A. et al. High-resolution photoemission on Sr_2RuO_4 reveals correlation-enhanced effective spin–orbit coupling and dominantly local self-energies. *Phys. Rev. X* **9**, 021048 (2019).
- Tyler, A. W., Mackenzie, A. P., Nishizaki, S. & Maeno, Y. High-temperature resistivity of Sr_2RuO_4 : bad metallic transport in a good metal. *Phys. Rev. B* **58**, R10107(R) (1998).
- Bergemann, C., Mackenzie, A. P., Julian, S. R., Forsythe, D. & Ohmichi, E. Quasi-two-dimensional Fermi liquid properties of the unconventional superconductor Sr_2RuO_4 . *Adv. Phys.* **52**, 639–725 (2003).
- Mravlje, J. et al. Coherence–incoherence crossover and the mass-renormalization puzzles in Sr_2RuO_4 . *Phys. Rev. Lett.* **106**, 096401 (2011).
- Wang, Y. et al. Global phase diagram of a spin-orbital Kondo impurity model and the suppression of Fermi-liquid scale. *Phys. Rev. Lett.* **124**, 136406 (2020).
- Horvat, A., Žitko, R. & Mravlje, J. Spin–orbit coupling in three-orbital Kanamori impurity model and its relevance for transition-metal oxides. *Phys. Rev. B* **96**, 085122 (2017).
- Dietl, C. et al. Tailoring the electronic properties of Ca_2RuO_4 via epitaxial strain. *Appl. Phys. Lett.* **112**, 031902 (2018).

54. Han, Q. & Millis, A. Lattice energetics and correlation-driven metal–insulator transitions: the case of Ca_2RuO_4 . *Phys. Rev. Lett.* **121**, 067601 (2018).
55. Gorelov, E. et al. Nature of the Mott transition in Ca_2RuO_4 . *Phys. Rev. Lett.* **104**, 226401 (2010).
56. Hao, H. et al. Metal–insulator and magnetic phase diagram of Ca_2RuO_4 from auxiliary field quantum Monte Carlo and dynamical mean field theory. *Phys. Rev. B* **101**, 235110 (2020).
57. Anisimov, V. I., Bukhvalov, D. & Rice, T. M. Electronic structure of possible nickelate analogs to the cuprates. *Phys. Rev. B* **59**, 7901–7906 (1999).
58. Chaloupka, J. & Khaliullin, G. Orbital order and possible superconductivity in $\text{LaNiO}_3/\text{LaMO}_3$ superlattices. *Phys. Rev. Lett.* **100**, 016404 (2008).
59. Benckiser, E. et al. Orbital reflectometry of oxide heterostructures. *Nat. Mater.* **10**, 189–193 (2011).
60. Kumah, D. P. et al. Tuning the structure of nickelates to achieve two-dimensional electron conduction. *Adv. Mater.* **26**, 1935–1940 (2014).
61. Fowlie, J. et al. Conductivity and local structure of LaNiO_3 thin films. *Adv. Mater.* **29**, 1605197 (2017).
62. Han, M. J., Wang, X., Marianetti, C. A. & Millis, A. J. Erratum: Dynamical mean-field theory of nickelate superlattices [Phys. Rev. Lett. **107**, 206804 (2011)]. *Phys. Rev. Lett.* **110**, 179904 (2013).
63. Disa, A. S. et al. Orbital engineering in symmetry-breaking polar heterostructures. *Phys. Rev. Lett.* **114**, 026801 (2015).
64. Li, D. et al. Superconductivity in an infinite-layer nickelate. *Nature* **572**, 624–627 (2019).
65. Först, M. et al. Nonlinear phononics as an ultrafast route to lattice control. *Nat. Phys.* **7**, 854–856 (2011).
66. Subedi, A., Cavalleri, A. & Georges, A. Theory of nonlinear phononics for coherent light control of solids. *Phys. Rev. B* **89**, 220301(R) (2014).
67. Rini, M. et al. Control of the electronic phase of a manganite by mode-selective vibrational excitation. *Nature* **449**, 72–74 (2007).
68. Disa, A. S. et al. Polarizing an antiferromagnet by optical engineering of the crystal field. *Nat. Phys.* **16**, 937–941 (2020).
69. Nova, T. E., Disa, A. S., Fechner, M. & Cavalleri, A. Metastable ferroelectricity in optically strained SrTiO_3 . *Science* **364**, 1075–1079 (2019).
70. Juraschek, D. M., Fechner, M. & Spaldin, N. A. Ultrafast structure switching through nonlinear phononics. *Phys. Rev. Lett.* **118**, 054101 (2017).
71. Gu, M. & Rondinelli, J. M. Nonlinear phononic control and emergent magnetism in Mott insulating titanates. *Phys. Rev. B* **98**, 024102 (2018).
72. Fausti, D. et al. Light-induced superconductivity in a stripe-ordered cuprate. *Science* **331**, 189–191 (2011).
73. Mankowsky, R. et al. Nonlinear lattice dynamics as a basis for enhanced superconductivity in $\text{YBa}_2\text{Cu}_3\text{O}_{6.5}$. *Nature* **516**, 71–73 (2014).
74. Mitrano, M. et al. Possible light-induced superconductivity in K_3C_{60} at high temperature. *Nature* **530**, 461–464 (2016).
75. Buzzi, M. et al. Photo-molecular high temperature superconductivity. *Phys. Rev. X* **10**, 031028 (2020).
76. Kennes, D. M., Wilner, E. Y., Reichman, D. R. & Millis, A. J. Transient superconductivity from electronic squeezing of optically pumped phonons. *Nat. Phys.* **13**, 479–483 (2017).
77. Denny, S. J., Clark, S. R., Laplace, Y., Cavalleri, A. & Jaksch, D. Proposed parametric cooling of bilayer cuprate superconductors by terahertz excitation. *Phys. Rev. Lett.* **114**, 137001 (2015).
78. Michael, M. H. et al. Parametric resonance of Josephson plasma waves: a theory for optically amplified interlayer superconductivity in $\text{YBa}_2\text{Cu}_3\text{O}_{6+x}$. *Phys. Rev. B* **102**, 174505 (2020).
79. Adler, R. et al. Correlated materials design: prospects and challenges. *Rep. Prog. Phys.* **82**, 012504 (2018).

Acknowledgements

C.A. acknowledges support from the US Department of Energy, Office of Science, Office of Basic Energy Sciences under award DE-SC0019211. S.I.-B. acknowledges support from the US Department of Defense Army Research Office under award ARO W911NF-19-1-0371 and the US National Science Foundation under awards NSF DMR-1838463 and NSF ACI-1339804. A.J.M. acknowledges support from NSF DMR-1420634, the Columbia University Center for Precision Assembly of Superstratic and Superatomic Solids. J.-M.T. acknowledges J. Fowlie for her help with the nickelate section, X. Ravinet for designing Fig. 1 and the Swiss National Science Foundation for support through Division II (project 200020_179155). A.C., A.G. and J.-M.T. acknowledge the support of the European Research Council under the European Union's Seventh Framework Programme (FP7/2007-2013)/ERC grant agreement 319286 Q-MAC. The Flatiron Institute (A.G., A.J.M.) is a division of the Simons Foundation.

Competing interests

The authors declare no competing interests.

Additional information

Correspondence should be addressed to S.I.-B.

Peer review information *Nature Materials* thanks the anonymous reviewers for their contribution to the peer review of this work.

Reprints and permissions information is available at www.nature.com/reprints.

Publisher's note Springer Nature remains neutral with regard to jurisdictional claims in published maps and institutional affiliations.

© Springer Nature Limited 2021